



<b><i>Publication Year</i></b>	2020
<b><i>Acceptance in OA</i></b>	2023-01-23T16:20:23Z
<b><i>Title</i></b>	Interstellar comet 2I/Borisov exhibits a structure similar to native Solar system comets
<b><i>Authors</i></b>	Manzini, F., Oldani, V., Ochner, P., BEDIN, Luigi
<b><i>Publisher's version (DOI)</i></b>	10.1093/mnrasl/slaa061
<b><i>Handle</i></b>	<a href="http://hdl.handle.net/20.500.12386/33012">http://hdl.handle.net/20.500.12386/33012</a>
<b><i>Journal</i></b>	MONTHLY NOTICES OF THE ROYAL ASTRONOMICAL SOCIETY. LETTERS
<b><i>Volume</i></b>	495

# Interstellar comet 2I/Borisov exhibits a structure similar to native Solar system comets

F. Manzini,<sup>1</sup>★ V. Oldani,<sup>1</sup> P. Ochner<sup>2,3</sup> and L. R. Bedin<sup>2</sup>★

<sup>1</sup>Stazione Astronomica di Sozzago, Cascina Guascona, I-28060 Sozzago (Novara), Italy

<sup>2</sup>INAF-Osservatorio Astronomico di Padova, Vicolo dell'Osservatorio 5, I-35122 Padova, Italy

<sup>3</sup>Department of Physics and Astronomy, University of Padova, Via F. Marzolo 8, I-35131 Padova, Italy

Accepted 2020 April 1. Received 2020 April 1; in original form 2019 November 22

## ABSTRACT

We processed images taken with the *Hubble Space Telescope* (*HST*) to investigate any morphological features in the inner coma suggestive of a peculiar activity on the nucleus of the interstellar comet 2I/Borisov. The coma shows an evident elongation, in the position angle (PA)  $\sim 0$ – $180^\circ$  direction, which appears related to the presence of a jet originating from a single active source on the nucleus. A counterpart of this jet directed towards PA  $\sim 10^\circ$  was detected through analysis of the changes of the inner coma morphology on *HST* images taken on different dates and processed with different filters. These findings indicate that the nucleus is probably rotating with a spin axis projected near the plane of the sky and oriented at PA  $\sim 100$ – $280^\circ$ , and that the active source is lying in a near-equatorial position. Subsequent observations of *HST* allowed us to determine the direction of the spin axis at right ascension (RA) =  $17^{\text{h}}20^{\text{m}} \pm 15^\circ$  and declination (Dec.) =  $-35^\circ \pm 10^\circ$ . Photometry of the nucleus on *HST* images of 2019 October 12 only spans  $\sim 7$  h, insufficient to reveal a rotational period. The morphology exhibited by the interstellar comet 2I/Borisov is very similar to that of comet C/2014 B1 suggesting that the activation processes are the same as those observed in the Solar system native comets.

**Key words:** comets: general – comets: individual (2I/Borisov).

## 1 INTRODUCTION

Comet 2I/Borisov is only the second interstellar object known to have passed through the Solar system (Guzik et al. 2019; Ye et al. 2019); it therefore provides an invaluable opportunity to investigate the structure and dust characteristics of small objects presumably formed in another, distant star system.

This comet was observed in images taken on 2019 September 10 and 13 with the *WHT* and *GNT* telescopes, when it showed only an extended coma and a faint, broad tail. The colour of the comet was slightly reddish with a  $(g' - r')$  colour index of  $0.66 \pm 0.01$  mag, compatible with Solar system comets. Its observed morphology was best explained by dust with a low ejection speed ( $44 \pm 14 \text{ m s}^{-1}$ ) for  $\beta = 1$  particles, where  $\beta$  is the ratio of the solar gravitational attraction to the solar radiation pressure (Guzik et al. 2020). Almost simultaneously, the comet was observed by D. Jewitt and J. Luu with the *NOT* telescope on six dates between September 13 and October 4, and the early results prompted D. Jewitt et al. to submit a successful DDT proposal to observe comet Borisov with the *Hubble Space Telescope* (*HST*). Some results were published in Jewitt & Luu (2019).

A total of 24 images of the comet, of 260 s each, were taken by the *HST* WFC3 camera in the F350LP broad-band filter (centred at 584.94 nm) on 2019 October 12 in four consecutive orbits. After they were released to the public, we could use them to perform an analysis of the morphology of the coma of the comet, which is the focus of this letter. Additional analyses were performed after release of new images taken by *HST* during single orbits on three successive dates: 2019 November 16 and December 9, and 2020 January 3.

## 2 METHODS

In order to perform a morphological analysis of the inner coma, where structures due to the emission of gas and dust from active sources on the nucleus are more easily detectable, we co-added and averaged separately the four series of six *HST* images of October 12. The comparative analysis of the four series did not show obvious structural variations over the  $\sim 7$  h imaging time span (from  $13^{\text{h}}44^{\text{m}}39^{\text{s}}$  UT to  $20^{\text{h}}42^{\text{m}}23^{\text{s}}$  UT of 2019 October 12); therefore, we decided to stack the four series of *HST* images in a single image corresponding to a total exposure of 6240 s (104 min), to obtain the highest possible signal-to-noise ratio.

To highlight the structures of the inner coma, we applied different algorithms, often used for this type of analysis: median subtraction,

\* E-mail: manzini.ff@aruba.it (FM); luigi.bedin@inaf.it (LRB)

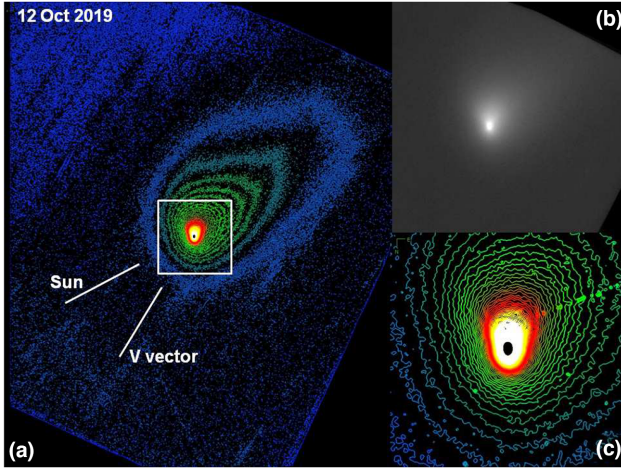


**Figure 1.** (a) Stacked *HST* image shown in isophote colour palette to highlight the shape and direction of the tail. The difference in brightness between each isophote is 75 ADU. The farthest blue isophote is just 20 ADU above the sky background. The length of the dust tail is 40 arcsec ( $8 \times 10^4$  km) on the sky plane. (b) Original *HST* image as in (a), 0.5 $\times$  resized. (c) Magnification of the area surrounding the nucleus [white box in (a), 10 arcsec side,  $2 \times 10^4$  km].

division by  $1/r$ , division by  $1/r^{1.2}$  (Samarasinha & Larson 2014), and Larson–Sekanina with  $30^\circ$  angle (Larson & Sekanina 1984). The comparison of the results of the four methods showed that the details highlighted were always the same in the same place; however, the latter process provided the highest signal-to-noise ratio.

We also applied false colour palette or isophote visualization to enhance the visibility of the details, as well as a polar transformation, centred on the optocentre, to the processed images, with the aim of highlighting and determining the precise position angle (PA) of any structures revealed by the processing algorithms. Knowing that the nominal resolution of the *HST* WFC3 camera is  $\sim 0.03977$  arcsec per pixel (Bellini, Anderson & Bedin 2011; Gennaro et al. 2018), corresponding to 81.1 km on the plane of the sky at the distance of the comet, it was then easy to convert the measured distances from pixels into km.

Finally, we also performed photometric measures of the nucleus on each of the original *HST* images to determine its instrumental magnitude. We applied the same parameters used by Bolin (2020): a photometric circle with a 5-pixel diameter (0.2 arcsec) centred on the comet’s optocentre (assumed to correspond to the nucleus) and an annulus with internal and external radii of 6 and 20 pixels (0.8 arcsec), respectively, to measure the mean background value.

### 3 ANALYSIS OF THE COMET

#### 3.1 Dust tail

The stacked *HST* image of October 12 was processed in isophote colour palette, to determine the shape and direction of the tail. We applied a brightness gap between each isophote as low as 75 ADU, ranging from 19307 ADU at the peak brightness of the comet’s nucleus to 1820 ADU of the farthest blue isophote, just 20 ADU above the sky background, in order to detect the faintest details (Fig. 1). The orientation of the tail appears to be approximately aligned with the antisolar vector in the image visualized with this method. Recently, Jewitt & Luu (2019) reported that the visible

portion of the tail is limited to about 60 arcsec in length by sky noise and field structures on images taken with Earth-based telescopes. However, in the stacked *HST* images, the farthest point where the end of the tail could be detected is about 970 pixels from the nucleus (40 arcsec), corresponding to a sky plane length  $L = 8.1 \times 10^4$  km and, assuming it is in antisolar direction, to an estimated true length  $L_T = 8.1 \times 10^4 \times \sin \alpha^{-1} = 2.4 \times 10^5$  km (with  $\alpha = 20^\circ$ , where  $\alpha$  is the phase angle as calculated with the JPL/HORIZON software<sup>1</sup>).

The high density of the isophotes in the area surrounding the nucleus (white–yellow–red isophotes, in Fig. 1c) suggests that the tail could partially originate from an almost isotropic distribution of dust, although the elongation of the inner coma is also suggesting a strong contribution of a radial emitting structure. On the contrary, the rapid decrease of the density of the isophotes moving away from the nucleus towards the end of the tail is indicative of a wide scattering of the emitted dust already at a relatively low distance from the nucleus.

The length of the tail can provide useful information about the size of the dust grains of which it is made. Within the tail, the dust and gas emitted from the nucleus are decoupled, and the only significant forces affecting the grain trajectories are the solar gravity and the radiation pressure. Both forces depend on the square of the heliocentric distance, but work in opposite directions (Vincent, Bönnhardt & Lara 2010). Their sum can be seen as a reduced solar gravity, and the motion of dusts follows the equation

$$m \times a = (1 - \beta) \times (\text{solar gravity}), \quad (1)$$

where  $\beta$  is the ratio (radiation pressure)/(solar gravity), and is inversely proportional to the size of the grains for particles larger than  $1 \mu\text{m}$  (Bohren, Huffman & Kam 1983).

We performed a two-dimensional simulation of the dust tail made by means of the Finson–Probstein diagram (Comet Toolbox by J.B. Vincent<sup>2</sup>) up to 120 d earlier than 2019 October 12 using different  $\beta$  (Fig. 2). Considering the approximations introduced, we obtained a length and shape of the tail in the numerical simulation corresponding to that measured on the *HST* image for values of  $\beta$  between 0.01 and 0.03; it can therefore be estimated that the dust grains in the distal tail have radii between 30 and 100  $\mu\text{m}$ .

#### 3.2 Coma

The composite *HST* image of 2019 October 12 clearly shows the comet as non-stellar and the inner coma anisotropic and elongated in the N–S direction ( $< 3$  arcsec or 75 pixels; Bolin 2020), in contrast with the projected direction of the tail that is oriented towards PA  $300^\circ$ . This elongation becomes more obvious and prominent in the composite image. The elongation appears to be related to the presence of a jet, which we could detect with all the spatial filters applied. At least part of the dust coma most likely originates from the emission of this jet, well visible directed towards PA  $180^\circ$  in the image processed with the Larson–Sekanina filter. The high resolution of the WFC3 camera shows no visible substructures of this jet, suggesting that it originates from a single active source on the nucleus of the comet (Fig. 3).

The emitted dust appears scattered at a relatively low distance from the nucleus and is soon deflected by the solar radiation pressure to merge into the tail. This appearance is indicative of a low ejection

<sup>1</sup><https://ssd.jpl.nasa.gov/horizons.cgi>

<sup>2</sup><http://www.comet-toolbox.com>

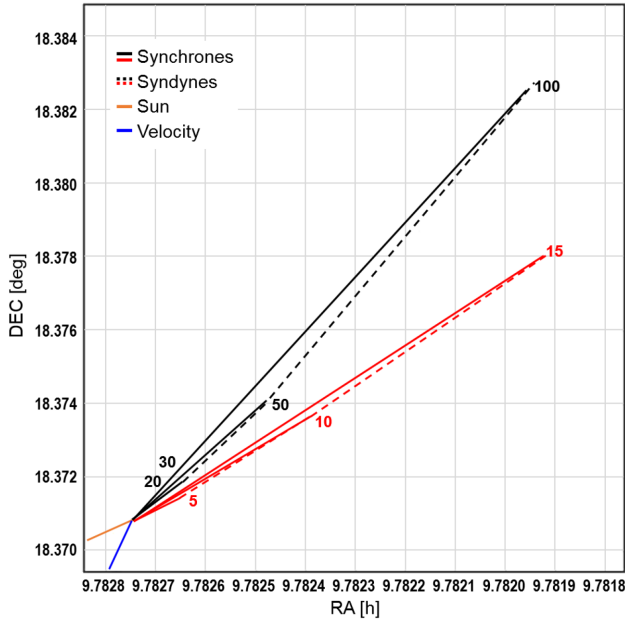


**Figure 2.** Two-dimensional modelling of the dust tail, made by means of the Finson–Probst diagram. The synchrones (black solid lines) and the syndynes (black dashed lines) originated from dust emissions of the nucleus occurred 15–100 d before 2019 October 12 are shown for  $\beta = 0.01$ . In red, the synchrones and syndynes from emissions 5–15 d before the same date for  $\beta = 0.3$ . For these higher  $\beta$  values, the model approximates the scattering of the dust as observed in the *HST* images.

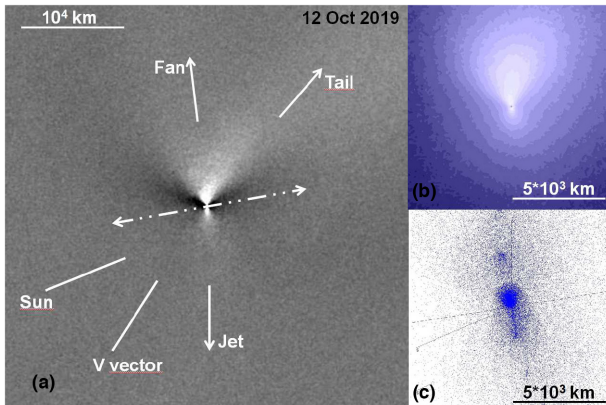


**Figure 3.** (a) *HST* image, processed with the Larson–Sekanina filter, showing the jet in PA 180° and the supposed position of the spin axis. (b) Same image, processed with  $1/r$  filter, visualized in isodensity contours. (c) Computer model of the morphology of the inner coma following the emission of dust from a single active area in equatorial position, showing features consistent with those observed in the *HST* images.

speed and possibly related to abundance of dust particles of a relatively small size.

We made further in-depth analysis in search for other structures in different PAs. Actually, we found a fan-shaped structure towards PA 10°, in a contralateral position with respect to the jet. The two structures are probably related, as they appear almost symmetrical on the opposite sides, thus most likely originating from the same single active source on a rotating nucleus (Fig. 4).

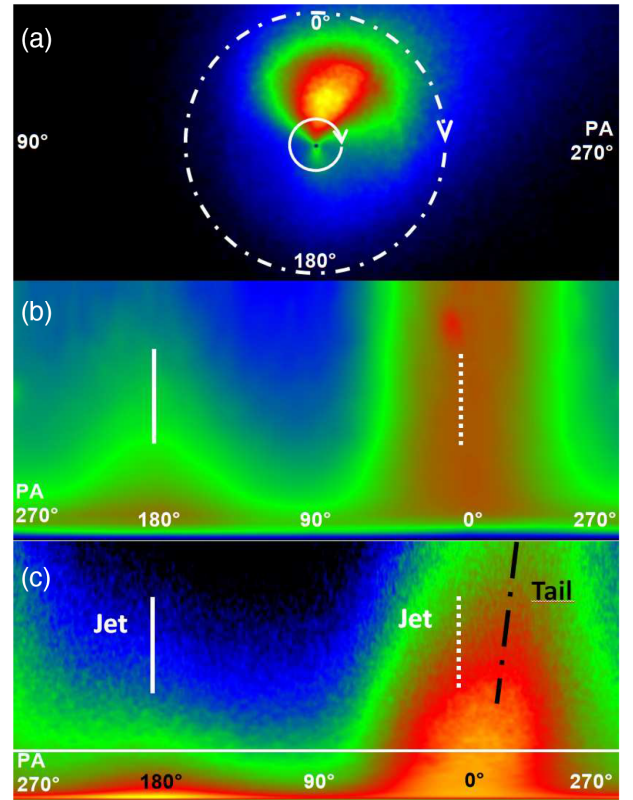


**Figure 4.** The original *HST* image processed with the  $1/r$  filter, shown in false colours in panel (a), was transformed in polar projection to identify the morphological details in the inner coma up to 30 pixels ( $2.4 \times 10^3$  km – solid white circle) and their PA (b). The brightest condensations at PA 180° and PA 10° correspond to the jets deriving from the emissions of a single active area. (c) Polar projection up to 150 pixels ( $1.2 \times 10^4$  km – dash and dot circle) shows the extent of the features on a wider scale and the development of the tail at a different PA than the jet.

### 3.3 Photometry of the nucleus

The images taken with *HST* are tracked at the differential motion rate of the comet with respect to the stars; therefore, we could only perform a photometry to determine the instrumental magnitude of the nucleus. The use of a small aperture (5-pixel diameter) of the photometric circle removes efficiently the diffuse light due to the dust in the coma and enables to detect the smallest variations in brightness due to discrete emissions related to the rotation of the nucleus (Lamy et al. 1998; Lamy, Toth & Weaver 1998). The measured instrumental magnitudes show small fluctuations suggestive of a possible period; however, the analysis made with standard algorithms based on the Fourier transforms and least-squares methods provided no evidence of that (Fig. 5).

## 4 DISCUSSION

### 4.1 Dust tail

Comet 2I/Borisov morphology looks similar to that of comet C/2014 B1 (Schwartz), with an equatorial ejection of dust particles from the nucleus and a near-equatorial viewing perspective (Jewitt et al. 2019). However, since comet C/2014 B1 was at about 9 au distance from the Sun, it showed a faint dust tail with a brightness just above the sky background, and only visible through isophote



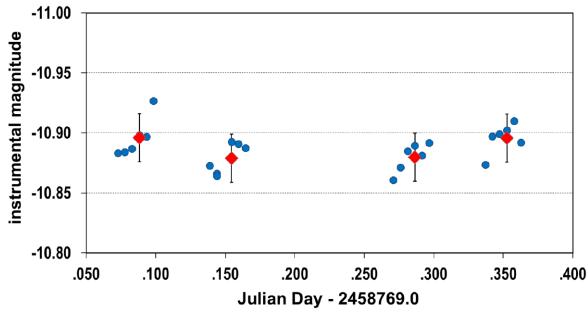


**Figure 5.** Photometry with instrumental values on the nucleus of 2I/Borisov performed on the original *HST* images taken on 2019 October 12 and spanning 7 h. The blue dots are the measurements of each image; the red diamonds are the calculated mean magnitude of each series of images.

visualization (see Fig. 7, available only as supplementary online material). On the contrary, comet 2I/Borisov is at much lower heliocentric distance and shows a greater emission of gas and dust. Here, solar gravity and solar radiation pressure are shaping the morphology of the dust coma, and its tail is in fact obvious and oriented in nearly antisolar direction. Dust emission in comet 2I/Borisov seems to be less collimated than C/2014 B1, with the dust particles widely scattered in antisolar direction, possibly due to the combination of a lower ejection speed and the effect of a greater radiation pressure. Our estimate of the size of dust particles in the range of 30–100  $\mu\text{m}$  radius is consistent with that recently reported by Jewitt & Luu (2019). However, it should be considered that in both cases the estimates apply to particles displaced to the end of the visible tail in order to reproduce its apparent length. In fact, using higher  $\beta$  values in the Finson–Probst diagram, in the region close to the nucleus the simulation approaches the wide scattering of the emitted dust observed in the *HST* images, which might be suggestive of the presence also of dust particles with a smaller size.

#### 4.2 An emissive rotating structure

Assuming that the nucleus of comet 2I/Borisov is rotating and that the geometric position of the spin axis is such to favour a prolonged insolation, the dust emission from a single source located on the sunlit hemisphere should be modulated by the insolation and the resulting features of the inner coma should provide indications on the orientation of the spin axis. In the case of two emissive structures with similar morphology that are observed in approximately opposite directions, it could be supposed that both originated from the same active source on a nucleus that is rotating with a spin axis coinciding with the axis of the angle between the two structures and, if so, that they would be more evident when their position corresponds to the projection on the plane of the sky for the greater condensation of material on the perpendicular to the view (Sekanina 1987).

The finding of a jet at PA  $180^\circ$  and of its counterpart at PA  $10^\circ$  suggests that the active area originating the structures is located in a near-equatorial position, and that the nucleus is probably rotating with a spin axis lying near the plane of the sky and geometrically oriented at PA  $\sim 100^\circ$  or PA  $\sim 100^\circ + 180^\circ$  (Fig. 3). Unfortunately, from the *HST* images it is not possible to determine the direction of rotation of the nucleus. To further verify our findings, we run a computer model of the inner coma using a proprietary software (P. Pellissier, 2009) specifically designed to reproduce Earth-based

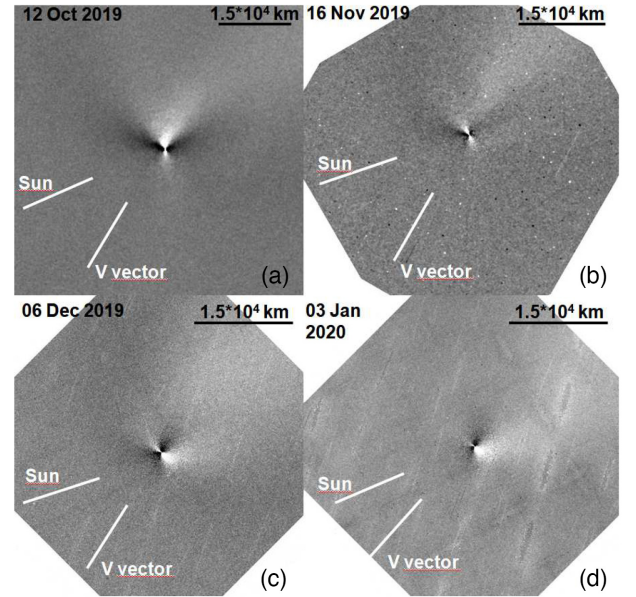


**Figure 6.** The *HST* images taken on four different dates have been processed with the same procedure. A Larson–Sekanina filter ( $\alpha = 45^\circ$ ) has been applied to highlight micro-contrasts in the inner coma. The jet visible in PA  $\sim 180^\circ$  on the first date becomes more and more evident over time, while the opposite happens for the contralateral structure in PA  $\sim 10^\circ$ . The direction of the spin axis (assumed as the bisector of the angle between the two structures) changes due to the variation of the geometric conditions of observation from Earth.

observations of the dust coma structures and of the development of the tail. The parameters needed to run the model are the properties of the dust particles, those of the nucleus, and the geometric conditions of the Sun–Earth–comet system. The following physical parameters of the dust particles, compatible with the observations of Rosetta on comet 67P (Fulle et al. 2015; Rotundi et al. 2015; Guettler et al. 2019), were entered in the model (albedo: 0.03; diameter: 50  $\mu\text{m}$ ; density: 0.6  $\text{g cm}^{-3}$ ; ejection velocity: 25  $\text{ms}^{-1}$ ; dispersion: 0.75). For the cometary nucleus (assumed spherical), we entered a latitude of  $5^\circ$  for a single jet at and a direction of the spin axis at PA  $100^\circ$ . Since the rotation period was not known, we run the model applying only three full rotations in order to simulate the early development of the inner coma features before they would be hidden by the dust. The resulting model is shown in Fig. 3(c). The features shown by the model are consistent with those observed in the *HST* image processed with spatial filters. By applying higher number of rotations to the nucleus, it was also possible to model the development of the tail, which appeared similar to that observed on the *HST* image.

Our findings gathered stronger evidence by analysis of new *HST* images taken in the subsequent dates, thanks to the changes in the geometric conditions of the observation (Fig. 6). In these images, the jet that appeared directed towards PA  $\sim 180^\circ$  on 2019 October 12 becomes more and more evident and subsequently takes the shape of a fan due to the variations of insolation. These findings also confirms the near-equatorial position of the emitting source and thus the rotation of the nucleus.

The availability of *HST* observations extended over a period of about 80 d has also allowed us to study the changes in the direction of the axis of the angle between the two observed jets, which remained lying on the plane of the sky, as confirmed by the fact that the jet never showed evolution into shells or bow-shaped structures

(Fig. 8, animation available only as supplementary online material). Assuming that the nucleus of the comet is spherical and that the active area is located within  $10^\circ$  latitude from the equator, by means of a trial-and-error analysis, we found the best fit for the direction of the spin axis at  $RA = 17^h 20^m \pm 15^\circ$  and  $Dec. = -35^\circ \pm 10^\circ$  (or in opposite direction).

The time span of only  $\sim 7$  h is too short to allow for a detection of a possible periodicity of the rotation of the cometary nucleus by means of a photometric analysis. In fact, no significant variations in the light curve on the same dates were detected also by Bolin (2020), who hypothesized that the coma of 2I/Borisov may be too compact to see the rotational variation of the nucleus, or that the nucleus itself is spherical, has slow rotation period, or is oriented with an unfavorable geometry. The same Author however, using the 14 orbit *HST* data-set from 2019 December 23–25, could see slight magnitude variations in the lightcurve, corresponding to a possible period of about 11 h, though he hypothesized that this small variation could be due to short-term changes in the activity of comet 2I/Borisov. Despite the intrinsic limitations of our measurements, we think that the small variations that we could detect in the instrumental magnitude suggest a confirmation that the nucleus is rotating, although a series of high-resolution images over a longer time period would be needed to confirm the comet's rotation period with sufficient accuracy.

## 5 CONCLUSIONS

From our analyses of the recent *HST* images of the interstellar comet 2I/Borisov, we found the following:

- (i) The comet is strongly emitting dust, and producing a tail that is approximately aligned with the antisolar vector with a sky plane length  $L = 8.1 \times 10^4$  km.
- (ii) Modelling of the tail suggests that the dust grains have radii between 30 and 100  $\mu\text{m}$ , although the wide scattering of the emitted dust might also be suggestive of the presence of smaller dust particles around the nucleus.
- (iii) A clear elongation of the peri-nuclear area appears related to the presence of a jet probably deriving from an active source in a near-equatorial position. At least part of the dust coma and part of the tail most likely originate from this jet.
- (iv) The nucleus is probably rotating with a spin axis lying near the plane of the sky and geometrically oriented at  $PA \sim 100^\circ$  or  $PA \sim 100^\circ + 180^\circ$  on 2019 October 12. The small variations detected in the instrumental magnitude values confirm this finding, although they do not allow to estimate a periodicity of the rotation of the nucleus.
- (v) The spin axis direction was determined at  $RA = 17^h 20^m \pm 15^\circ$  and  $Dec. = -35^\circ \pm 10^\circ$ .

In summary, the preliminary findings of our analyses suggest that the interstellar comet 2I/Borisov appears similar in morphology and behaviour to the native Solar system comets.

## ACKNOWLEDGEMENTS

Based on observations with the NASA/ESA *Hubble Space Telescope*, obtained at the Space Telescope Science Institute, which is operated by AURA, Inc., under NASA contract NAS 5-26555. LRB acknowledges partial support by MIUR under PRIN program #2017Z2HSMF.

## REFERENCES

- Bellini A., Anderson J., Bedin L. R., 2011, *PASP*, 123, 622  
 Bohren C. F., Huffman D. R., Kam Z., 1983, *Nature*, 306, 625  
 Bolin B. T., 2020, preprint ([arXiv:1912.07386](https://arxiv.org/abs/1912.07386))  
 Fulle M. et al., 2015, *ApJ*, 802, L12  
 Gennaro M. et al., 2018, WFC3 Data Handbook, <http://www.stsci.edu/hst/wfc3> (accessed 2020 March 28)  
 Guettler C. et al., 2019, *A&A*, 630, A24  
 Guzik P., Drahus M., Rusek K., Waniak W., Cannizzaro G., Pastor-Marazuela I., 2019, *Astron. Telegram*, 13100  
 Guzik P., Drahus M., Rusek K., Waniak W., Cannizzaro G., Pastor-Marazuela I., 2020, *Nat. Astron.*, 4, 53  
 Jewitt D., Luu J., 2019, *ApJ*, 886, L29  
 Jewitt D., Kim Y., Luu J., Graykowski A., 2019, *AJ*, 157, 103  
 Lamy P., Toth I., Jorda L., Weaver H. A., A'Hearn M., 1998, *A&A*, 335, L25  
 Lamy P., Toth I., Weaver H., 1998, *A&A*, 337, 945  
 Larson S. M., Sekanina Z., 1984, *AJ*, 89, 571  
 Rotundi A. et al., 2015, *Science*, 347, 6220  
 Samarasinha N., Larson S. M., 2014, *Icarus*, 239, 168  
 Sekanina Z., 1987, in *ESA: Proceedings of the International Symposium on the Diversity and Similarity of Comets*. ESA, Noordwijk, p. 315  
 Vincent J. B., Bönnhardt H., Lara L. M., 2010, *A&A*, 512, A60  
 Ye Q. et al., 2020, *AJ*, 159, 77

## SUPPORTING INFORMATION

Supplementary data are available at *MNRAS* online.

**F7.ps**

**F8.mp4**

Please note: Oxford University Press is not responsible for the content or functionality of any supporting materials supplied by the authors. Any queries (other than missing material) should be directed to the corresponding author for the article.

This paper has been typeset from a  $\text{\LaTeX}$  file prepared by the author.